

Submitted to the Astrophysical Journal

The GeV-TeV Connection in Galactic γ -ray sources

S. Funk¹, O. Reimer², D. F. Torres³, J. A. Hinton⁴

ABSTRACT

Recent observations with atmospheric Cherenkov telescope systems such as H.E.S.S. and MAGIC have revealed a large number of new sources of very-high-energy (VHE) γ -rays from 100 GeV – 100 TeV, mostly concentrated along the Galactic plane. At lower energies (100 MeV – 10 GeV) the satellite-based instrument EGRET revealed a population of sources clustering along the Galactic Plane. Given their adjacent energy bands a systematic correlation study between the two source catalogues seems appropriate. Here, the populations of Galactic sources in both energy domains are characterised on observational as well as on phenomenological grounds. Surprisingly few common sources are found in terms of positional coincidence and spectral consistency. These common sources and their potential counterparts and emission mechanisms will be discussed in detail. In cases of detection only in one energy band, for the first time consistent upper limits in the other energy band have been derived. The EGRET upper limits are rather unconstraining due to the sensitivity mismatch to current VHE instruments. The VHE upper limits put strong constraints on simple power-law extrapolation of several of the EGRET spectra and thus strongly suggest cutoffs in the unexplored energy range from 10 GeV – 100 GeV. Physical reasons for the existence of cutoffs and for differences in the source population at GeV and TeV energies will be discussed. Finally, predictions will be derived for common GeV–TeV sources for the upcoming GLAST mission bridging for the first time the energy gap between current GeV and TeV instruments.

¹Kavli Institute for Particle Astrophysics and Cosmology (KIPAC), SLAC, CA 94025, USA. funk@slac.stanford.edu

²Stanford University, W. W. Hansen Experimental Physics Lab (HEPL) and KIPAC, Stanford, CA 94305-4085, USA. olr@stanford.edu

³ICREA & Institut de Ciències de l'Espai (IEEC-CSIC) Campus UAB, Fac. de Ciències, Torre C5, parell, 2a planta, 08193 Barcelona, Spain. dtorres@aliga.ieec.uab.es

⁴School of Physics and Astronomy, University of Leeds, Leeds LS2 9JT, UK. jah@ast.leeds.ac.uk

Subject headings: gamma rays: observations; Galaxy: general; (ISM:) supernova remnants

1. Introduction

In recent years the knowledge of the Galactic VHE γ -ray sky above 100 GeV has been greatly improved through the detection and subsequent study of many sources, mostly by means of ground-based Imaging Atmospheric Cherenkov telescope systems such as the High Energy Stereoscopic System (H.E.S.S.) or the Major Atmospheric Gamma-ray Imaging Cherenkov Observatory (MAGIC). Currently known Galactic VHE γ -ray emitters include shell-type Supernova remnants (SNRs) (Aharonian et al. 2006a, 2007a,b), Pulsar Wind Nebulae (PWNe) (Aharonian et al. 2005a, 2006b,c), γ -ray binaries (Aharonian et al. 2006d; Albert et al. 2006), Molecular clouds (Aharonian et al. 2006e) and possibly also clusters of massive stars (Aharonian et al. 2007c). These various source classes were discovered both in pointed observations using H.E.S.S. and MAGIC as well as in a systematic survey of the inner Galaxy performed with the H.E.S.S. instrument. The highest energy photons detected from these source classes reach ~ 100 TeV (Aharonian et al. 2007a), currently representing the end of the observable electromagnetic spectrum for astrophysical objects. It is natural to investigate the relationship of these TeV sources to sources at lower energies as will be done in this work focusing on Galactic sources. The closest energy band for which data exist is that studied by the Energetic Gamma Ray Experiment Telescope (EGRET) aboard the Compton Gamma-Ray Observatory with an energetic coverage from 100 MeV – 10 GeV (Hartman et al. 1999). The GeV sky has a distinctively different overall appearance compared to TeV energies. In particular focusing on our Galaxy, the most prominent feature of the GeV sky is the dominant diffuse emission from cosmic ray (CR) interactions in the Galaxy, while the TeV sky due to the steeply falling energy spectrum of the diffuse component is dominated by individual sources. However, several prominent γ -ray sources are known to emit at both GeV and at TeV energies, the Crab Nebula being the most prominent example (Weekes et al. 1989; Nolan et al. 1993; Aharonian et al. 2004, 2006f; Albert et al. 2007a).

In this paper the relationship between Galactic EGRET and VHE γ -ray sources will be assessed in a systematic way. For cases with a positional coincidence between a VHE and an EGRET source (in the following called “coincident sources”) all currently known Galactic objects will be considered. For cases in which a source is detected only in one band – the “non-coincident sources” – we focus on the region covered by the H.E.S.S. Galactic plane survey (GPS) during 2004 and 2005 (Aharonian et al. 2005b, 2006g) (Galactic longitude

$\pm 30^\circ$, Galactic latitude $\pm 3^\circ$) so that a statistical assessment of the “non-connection” can be made. EGRET was unable to perform detailed studies of the γ -ray sky above 10 GeV, partly due to back-splash of secondary particles produced by high-energy γ -rays causing a self-veto in the monolithic anti-coincidence detector used to reject charged particles. The upcoming Gamma Ray Large Area Space Telescope (GLAST) Large Area Telescope (LAT) will not be strongly affected by this effect since the anti-coincidence shield was designed in a segmented fashion (Moiseev et al. 2007). Moreover, the effective area of the GLAST-LAT will be roughly an order of magnitude larger than that of EGRET. The GLAST-LAT mission will therefore for the first time fully bridge the gap between the energy range of EGRET and current VHE instruments. Part of the study presented here can be seen as preparatory work for GLAST-LAT studies of sources in the largely unexplored energy band between 10 and 100 GeV.

From the 2004 and 2005 H.E.S.S. GPS 22 VHE γ -ray sources have been reported in the Inner Galaxy. The third EGRET catalogue (Hartman et al. 1999) represents the companion to the VHE source catalogue above an energy threshold of 100 MeV (with peak sensitivity between 150 and 400 MeV, depending on the γ -ray source spectrum). It lists 271 sources, 17 of which are located within the H.E.S.S. GPS region. Whilst the EGRET range currently represents the nearest energy band to VHE γ -rays, for the very few EGRET sources detected all the way up to ~ 10 GeV, there is still an unexplored energy band of roughly one decade before the VHE γ -ray energy range begins at ~ 100 GeV (it should be noted that EGRET does have some sensitivity beyond 10 GeV: Thompson, Bertsch & O’Neal (2005) reported the detection of ~ 1500 photons above that energy with 187 of these photons being found within 1° of a source listed in the third EGRET catalogue). Comparing the instrumental parameters of VHE instruments and EGRET there is a clear mismatch both in angular resolution and in sensitivity as can be seen in Figure 1. In a ~ 5 hour observation (as a typical value in the GPS region) H.E.S.S. is a factor of $\sim 50 - 80$ more sensitive (in terms of energy flux $E^2 dN/dE$) than EGRET above 1 GeV in the Galactic Plane for the exposure accumulated between 1991 and 1995 (corresponding to the third EGRET catalogue). Assuming a similar energy flux output in the two different bands this mismatch implies at first sight that H.E.S.S. sources are not likely to be visible in the EGRET data set. Conversely (again under the assumption of equal energy flux output), VHE γ -ray instruments should be able to detect the majority of the EGRET sources, as has been suggested in the past. Figure 2 compares the energy fluxes $\nu F \nu$ for EGRET sources and H.E.S.S. sources in the inner Galaxy. Clearly, the EGRET sources do not reach down as low in energy flux as the H.E.S.S. sources, a picture that will change once the GLAST-LAT is in orbit as depicted by the GLAST-LAT sensitivity (dashed line). In reality the naïve expectation of equal energy flux output in the GeV and TeV band can easily be wrong in Galactic γ -ray sources for

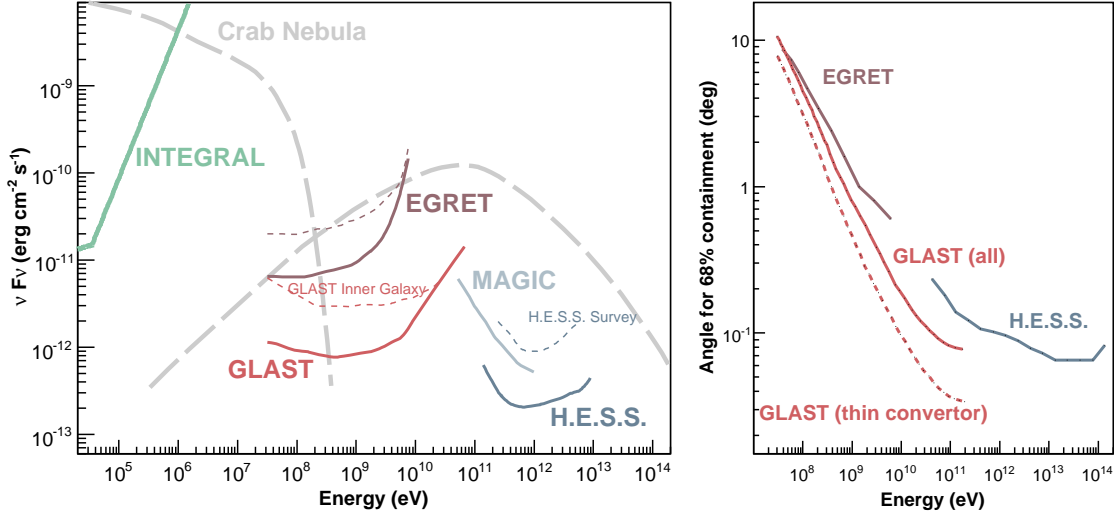


Fig. 1.— **Left:** Integral sensitivities for current, past and future γ -ray instruments ($5\text{-}\sigma$ sensitivity for $E > E_0$ multiplied with E_0 assuming a spectrum of E^{-2}). The solid lines show the nominal instrument sensitivities (for a typical observation time as specified below), the dashed curves show the actual sensitivities for the Inner Galaxy as appropriate for this work. INTEGRAL’s (IBIS/ISGRI) sensitivity curve (solid green) shows the sensitivity for an observation time of 10^5s , a typical value in the Inner Galaxy. The EGRET curves (brown) are shown for the whole lifetime of the mission (periods 1–9) for the Galactic anti-centre (solid) which received the largest exposure time and has a lower level of diffuse γ -ray emission than the Inner Galaxy and for the position of RX J1713.7–3946 (dashed), a typical position in the Inner Galaxy dominated by diffuse γ -ray background emission. The GLAST curves in red (taken from http://www-glast.slac.stanford.edu/software/IS/glast_lat_performance.html) show the 1-year sky-survey sensitivity for the Galactic North pole – again a position with low diffuse emission (solid), and for the position of RX J1713.7–3946 (dashed). The H.E.S.S. curves (blue) are shown for a 50-hour pointed observation of a point-like source (solid) and for a 5-hour observation of a somewhat extended source as is typical for the Galactic Plane survey (angular cut of $\sqrt{0.05}$). The MAGIC curve (light blue) represents a 50-hour observation of a point-source. **Right:** Energy-dependence of the angular resolution for selected γ -ray instruments expressed by the 68%-containment radius of the point-spread function (PSF). As can be seen, the angular resolution of GLAST becomes comparable with current VHE instruments at high energies, whilst at the lower energy end GLAST and EGRET have comparable resolutions.

various reasons: EGRET sources may not emit comparable energy fluxes in the VHE γ -ray band but rather exhibit cut-offs or spectral breaks in the energy band between EGRET and H.E.S.S. (this is certainly the case for pulsed magnetospheric emission from pulsars, see for example Aharonian et al. 2007d). Furthermore, H.E.S.S.-like instruments are typically only sensitive to emission on scales smaller than $\sim 1^\circ$. If any of the EGRET sources are extended beyond 1° without significant sub-structure on smaller scales (not precluded given the poor angular resolution of EGRET), current Imaging Cherenkov instruments may not be able to detect them since these sources would completely fill the field of view (FoV) and be removed by typical background subtraction methods (see for example Berge, Funk & Hinton 2007). Given the upcoming launch of GLAST and the recent H.E.S.S. survey it seems timely to study the relationship between GeV and TeV emitting sources in more detail.

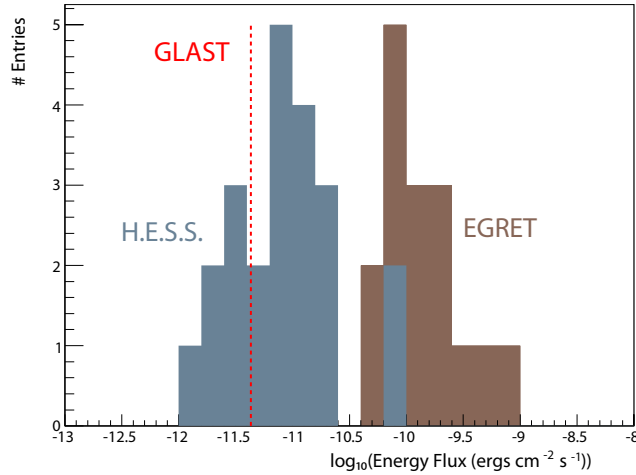


Fig. 2.— Distribution of integrated energy flux $\nu F \nu$ for sources in the Inner Galaxy discussed here. For EGRET the energy flux between 1 GeV and 10 GeV, for the H.E.S.S. sources, the energy flux between 1 TeV and 10 TeV is shown. Also shown is the sensitivity prediction for the GLAST-LAT for a typical location in the Inner Galaxy ($l=10$, $b=0$).

Section 2 describes the data and analysis methods used in this study, section 3 describes the sources detected in both energy bands, and section 4 focuses on sources detected in only one of the two energy regimes. In section 5 astrophysical implications of the study are discussed.

2. Analysis methods

For the sources discussed in this study locations and source spectra in the EGRET band (Hartman et al. 1999) and in the VHE γ -ray band are required. For the inner Galaxy, dedicated upper limits at the specific position of the γ -ray sources in the respective other band were determined. For the EGRET data these upper limits (at 1 GeV) were derived at the nominal positions of the H.E.S.S. sources based on a reanalysis of the data used for the production of the third EGRET catalogue, applying the standard EGRET likelihood fitting technique (Mattox et al. 1996). For the H.E.S.S. data, 2σ upper limits at the nominal position of each EGRET source were estimated. This was done by scaling the flux corresponding to the H.E.S.S.-point-source sensitivity in 25 hours (1% of the Crab) by the square-root of the ratio of 25 hours to the published exposure time at the position of the EGRET source (taken from Aharonian et al. 2006g).

2.1. Quantifying Positional Coincidence

Figure 3 shows all H.E.S.S. and all EGRET sources within the HESS GPS region. One property of EGRET and VHE γ -ray sources becomes immediately apparent: only a minor fraction of the H.E.S.S. sources coincide within the considerably larger location uncertainty contours of EGRET GeV sources. Given the rather poor angular resolution of EGRET (68% containment radius of the PSF: 1.5° at 1 GeV) coupled with typically rather limited photon statistic any systematic assessment of positional matches between EGRET and H.E.S.S. sources is dominated by the localisation error on the EGRET source position. The likelihood source position uncertainty contour (PUC) as given in Hartman et al. (1999) have been used to check for VHE γ -ray sources within these regions on the sky. While most of the VHE sources are extended, their extension is rather small on the scale of the EGRET positional uncertainty and therefore a source is classified as “coincident” if the centre of gravity of the VHE emission is within the EGRET likelihood PUC. For large sources such as e.g. the SNR RX J1713.7–3946 (HESS J1713–395) this approach is clearly an oversimplification, albeit it is the one used at this stage of this study.

The number of spatially coincident sources depends on the EGRET PUC chosen in the investigation. For the H.E.S.S. GPS-region, no VHE γ -ray source is located within the 68% positional confidence contour of any EGRET source. Relaxing the coincidence criterion, two VHE γ -ray sources are found within the 95%-confidence contour of EGRET source positions (shown in red in Figure 3) and an additional three VHE γ -ray sources are located within the 99%-confidence contours (shown in orange in Figure 3). Outside the H.E.S.S. GPS-region, no systematic statistical assessment of the non-coincident sources is possible due to

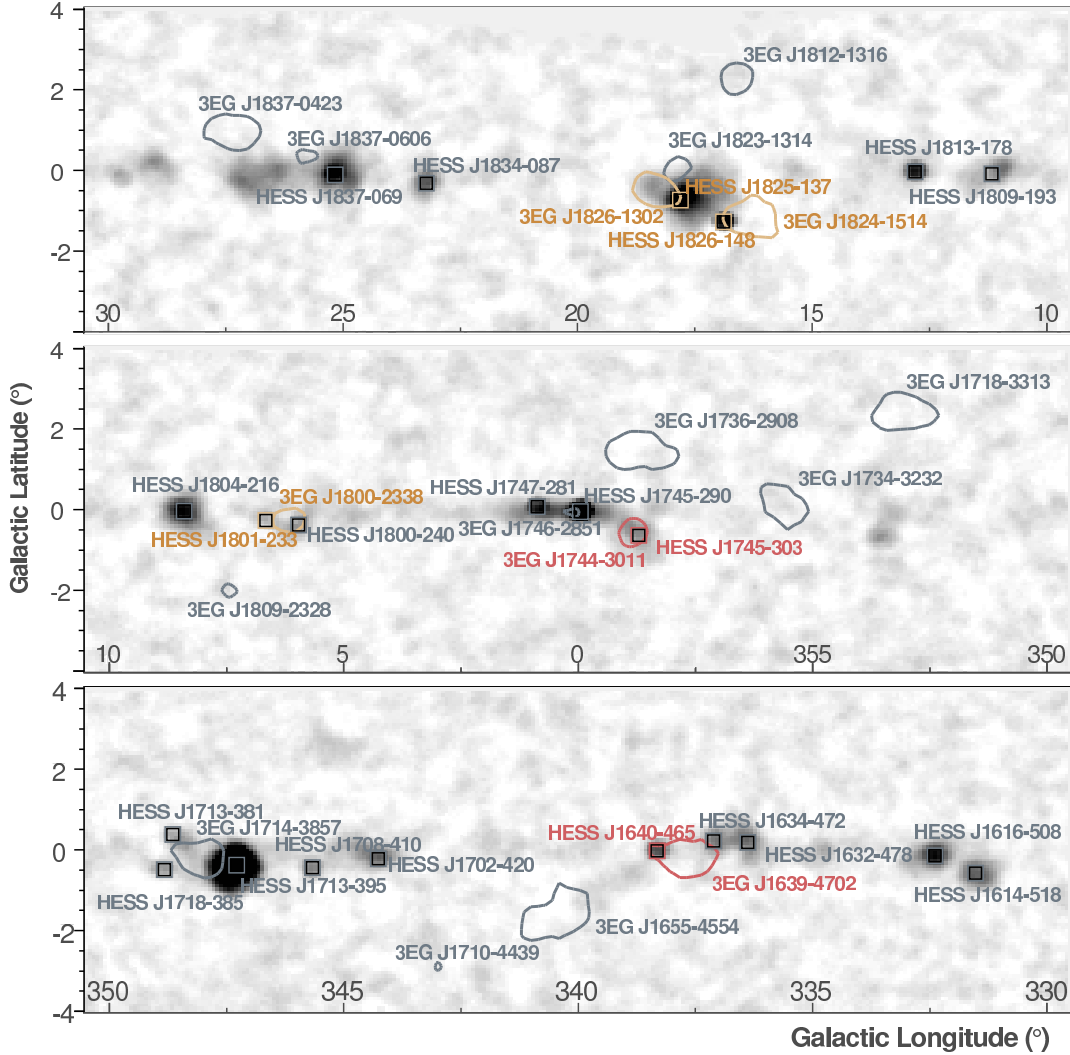


Fig. 3.— Map of the H.E.S.S. GPS region taken from Aharonian et al. (2006g). Published H.E.S.S. sources are marked as squares. EGRET sources are shown with their 95% positional confidence contours from the 3EG-catalogue. The red (orange) contours and labels denote those 3EG sources for which a H.E.S.S. source centroid is located within the 95% (99%) confidence contour, the blue contours denote the 95% PUCs for the EGRET sources for which no VHE emission is detected.

the highly non-uniform exposure of the observations with the limited-FoV VHE instruments. Nevertheless, it is relevant to note that four additional coincident sources are found outside the H.E.S.S. GPS-region within the Galactic plane (defined here as a latitude range of

EGRET Source	VHE γ -ray Source		
	Within 68% PUC	Within 95% PUC	Within 99% PUC
	Within the H.E.S.S. GPS		
3EG J1639–4702	None	HESS J1640–465	HESS J1800–233 HESS J1826–148 HESS J1825–137
3EG J1744–3011		HESS J1745–303	
3EG J1800–2338			
3EG J1824–1514			
3EG J1826–1302			
	Outside the H.E.S.S. GPS		
3EG J0241+6103	HESS J1420–607	None	MAGIC J0240+613
3EG J0617+2238			MAGIC J0616+225
3EG J0634+0521			HESS J0632+058
3EG J1420–6038			

Table 1: Positionally coincident EGRET and H.E.S.S. sources within our Galaxy for three confidence levels (68%, 95%, and 99%) of the positional uncertainty of the EGRET source.

$\pm 3^\circ$): HESS J1420–608 (Aharonian et al. 2006c) in the Kookaburra region is located within the 68% confidence contour of 3EG J1420–6038. The other three coincident Galactic sources are located within the 99% confidence contours of EGRET sources. The Crab Nebula is not listed in Table 2 although it has been detected by EGRET (Nolan et al. 1993) as well as by all major VHE γ -ray instruments (Weekes et al. 1989; Atkins et al. 2003; Aharonian et al. 2004, 2006f; Albert et al. 2007a). The reason for this is that in the 3EG catalogue only the position of the Crab pulsar is given, whereas the PUC of the off-pulse emission (i.e. the Nebula emission) has not been published thus far.

These coincident cases are discussed further in section 3. Table 1 summarises the VHE γ -ray sources located within EGRET confidence contours inside and outside the H.E.S.S. GPS region. Within the Galactic Plane survey region 17.1 square degrees (corresponding to 3% of the total GPS region) are covered by the EGRET 95%-confidence contours. Randomising the distribution of H.E.S.S. sources in the region (flat in longitude; Gaussian shape in latitude with a mean of -0.2° and a width of 0.34° as shown in Aharonian et al. 2006g) the probability for spatial coincidence between these two populations can be established. For the 95% confidence contours ~ 1.4 coincidences between the H.E.S.S.-source population and the EGRET sources is expected. The probability of detecting 2 or more sources when 1.4 sources are expected by chance is 40%, i.e. the positional coincidences could well be expected even

if the two population of sources are not related. Considering the (smaller) 68% confidence contours ~ 0.5 chance coincidences are expected; the probability for no coincidence when 0.5 are expected is 60%. For the (larger) 99% confidence contours the picture is similar: ~ 2.5 chance coincidences are expected; the probability of finding 5 coincidences when 2.5 are expected is $\sim 9\%$. Summarising these numbers, it is well possible within the statistics and properties of the two source classes that all the positional coincidences between H.E.S.S. and EGRET sources are chance coincidences. The numbers derived here do not strongly suggest common sources between the GeV and the TeV band, although it is (obviously) not precluded that the coincidences found point to real physical associations.

2.2. Determining Spectral Compatibility

Besides the test for positional coincidence a test of spectral compatibility, based on the simple assumption of a spectral extrapolation by a single power-law between the EGRET and the H.E.S.S. ranges has been performed. To assess the spectral match the quantity σ_{comb} has been defined in the following way:

$$\sigma_{\text{comb}} = \sqrt{\sigma_{\text{3EG}}^2 + \sigma_{\text{H.E.S.S.}}^2} \quad (1)$$

To determine σ_{3EG} , the spectral index of the EGRET source has been varied (around the pivot point of the EGRET best fit) until the extrapolation to 1 TeV matches the H.E.S.S. flux at that energy. This pivot point of the EGRET best fit is the energy at which the error on the index becomes independent from the error on the normalisation. This resulting index is called Γ_{match} and

$$\sigma_{\text{3EG}} = (\Gamma_{\text{match}} - \Gamma_{\text{3EG}})/(\Delta\Gamma_{\text{3EG}}) \quad (2)$$

(where Γ_{3EG} and $\Delta\Gamma_{\text{3EG}}$ is the EGRET index and its error taken from Hartman et al. 1999). Consequently, σ_{3EG} is a quantity that describes by how much the EGRET index has to be altered (with respect to the error on this index) to match the H.E.S.S. spectrum at 1 TeV. In the same way $\sigma_{\text{H.E.S.S.}}$, is determined by changing the H.E.S.S. spectral index until the flux matches the EGRET flux at 1 GeV (to avoid biases due to spectral cut-offs at the high end of the H.E.S.S. energy range the spectra were fitted only below 1 TeV in cases with clear spectral curvature). The two quantities σ_{3EG} and $\sigma_{\text{H.E.S.S.}}$ are finally added in quadrature to yield σ_{comb} , describing how well the two spectra can be extended into each other by a linear extrapolation. It should be noted that for the procedure described here, only the statistical (not the systematic) errors on the spectral indices are taken into account. For cases with a source detection only in one band, the same procedure can be applied using the upper limit in the other band (with the obvious difference that only the extrapolation from the source

spectrum onto the upper limit can be performed, not the other way around). For cases in which the power-law extrapolation with the nominal source photon index turns out to be lower – and therefore non-constraining – to the upper limit the corresponding measure $\sigma_{3\text{EG}}$ or $\sigma_{\text{H.E.S.S.}}$ is set to zero (i.e. the spectra are compatible). In several (but not the majority of) cases the EGRET spectrum can be preferentially fit by a higher order spectral shape (e.g. an exponential cutoff or a broken power-law) as will be discussed in section 4.

3. VHE γ -ray sources with EGRET counterparts

Only a few coincident sources between the GeV and the TeV band have been reported so far. The VHE γ -ray sources that positionally coincide with EGRET sources are summarised in Table 1. Whilst the positional coincidences between EGRET and VHE γ -ray sources might all be chance coincidences as shown in the previous section, in the following all positional coincidences within the 99% EGRET PUCs will be considered. Some of the properties of the sources and their respective source classes will be discussed along with an investigation on their spectral compatibility as introduced in the previous section.

3.1. Source Classes

For EGRET sources in the Galactic plane, the only firm identifications with sources at other wavelengths are for pulsars, based on matching radio or X-ray periodicity (Thompson et al. 1994). For many of the remaining Galactic EGRET sources, counterparts have been suggested, but the angular resolution of the instrument and the strong diffuse γ -ray background in the Galactic plane prevented unambiguous identifications. In VHE γ -rays, several source classes have been firmly identified as has been discussed e.g. in Funk (2006), based on matching morphology, positional coincidence or periodicity. However, the majority of Galactic VHE γ -ray sources also remain unidentified. Table 2 summarises potential counterparts of VHE sources in the coincident cases. While some of these identifications are rather solid (as e.g. in the case of the γ -ray binaries LS 5039 (Aharonian et al. 2006d) and LSI +61 303 (Albert et al. 2006)), in most of the other cases the identification of (even) the VHE γ -ray sources (with relatively small PUC of $\sim 1'$) lack any evidence of association beyond positional coincidence. In the cases where a firm identification exists, the VHE γ -ray source can be used to shed light on the nature of GeV source, assuming a physical relationship as shown for the Kookaburra region (Reimer & Funk 2007). Such studies demonstrate that observations with VHE γ -ray instruments can provide templates necessary to pin down the nature of unidentified EGRET γ -ray sources with suggestive but unproven counterparts.

With the upcoming advent of the GLAST-LAT instrument this approach will become very useful for associating the GeV emission as measured by a large-aperture space-based γ -ray instrument with narrow FoV but superior spatial resolution observations of ground-based VHE γ -ray instruments. Provided that the physical associations discussed in this section and shown in Table 2 are confirmed (as e.g., through more sensitive measurements with GLAST-LAT), three long-suspected classes of Galactic GeV sources (SNRs, PWNe and Binary systems) could finally be conclusively established. In the following these different source classes will be briefly discussed in the context of this study.

EGRET source	VHE γ -ray source	Potential Counterpart
Within the H.E.S.S. GPS		
3EG J1639–4702	HESS J1640–465	G338.3–0.0 (SNR/PWN)
3EG J1744–3011	HESS J1745–303	
3EG J1800–2338	HESS J1801–233	W28 (SNR)
3EG J1826–1302	HESS J1825–137	G18.0–0.7 (PWN)
3EG J1824–1514	HESS J1826–148	LS 5039 (Binary)
Outside the H.E.S.S. GPS		
3EG J0241+6103	MAGIC J0240+613	LSI +61 303 (Binary)
3EG J0617+2238	MAGIC J0616+225	IC443 (SNR/PWN)
3EG J0634+0521	HESS J0632+058	Monoceros
3EG J1420–6038	HESS J1420–607	Kookaburra (PWN)

Table 2: Coincident sources and potential counterparts to the VHE γ -ray sources (and hence also to the associated EGRET sources). The counterparts are classified into the source classes shell-type SNRs, PWNe and γ -ray binaries.

3.1.1. Pulsar wind nebulae

PWNe are currently the most abundant class amongst the identified Galactic VHE γ -ray sources, it is not therefore surprising that PWN are found as potential counterparts to the coincident sources. The first example for a coincident PWN is HESS J1825–137 – located within the 99% confidence region of 3EG 1826–1302. This source (Aharonian et al. 2006b) is currently the best-known example for an offset γ -ray PWN and as such represents a prototype for a new class of γ -ray sources. HESS J1825–137 shows a steepening of the energy spectrum with increasing distance from the central pulsar. This property, as well as the observed difference in size between the VHE γ -ray emitting region and the X-ray PWN associated with the pulsar PSR B1823–13 (Gaensler et al. 2003) can be naturally explained

by different cooling timescales for the radiating electrons of different energies. In this regard it will be important to study this region with the GLAST-LAT in the GeV band to confirm (or refute) this picture. Another example of VHE γ -ray PWN is HESS J1420–607, one of two likely PWN in the previously discussed Kookaburra region, which is located within the 68% confidence region of 3EG J1420–6038. The Crab Nebula is not listed in Table 2 although being a prominent GeV and TeV source because no position for the Crab off-pulse (nebular) emission has been published for the GeV data. For previously unidentified sources such as HESS J1640–465 (G338.3–0.0) an association with the X-ray PWN (Funk et al. 2007) is suggestive but not firmly established at this point.

3.1.2. *Shell-type Supernova remnants*

Shell-type SNRs constitute another prominent class of VHE γ -ray sources. However, the two most prominent VHE γ -ray shell-type SNRs RX J1713.7–3946 and RX J0852.0–4622 (Vela Jr.) are not prominent GeV emitters even though they are (up to now) the brightest steady VHE γ -ray sources in the sky after the Crab Nebula. Also Cas A and RCW 86 have been reported as VHE γ -ray sources (Aharonian et al. 2001; Albert et al. 2007c; Hoppe et al. 2007) but have not been detected by EGRET. Sturmer & Dermer (1995); Esposito et al. (1996); Romero, Benaglia, & Torres (1999); Torres et al. (2003) assessed the relationship between unidentified EGRET sources at low Galactic latitude and SNRs and found a statistically significant correlation between the two populations at the 4–5 σ level, were however not able to firmly and uniquely identify individual SNRs as EGRET sources. The GLAST-LAT will shed more light on the GeV emission in this source as well as in the whole population of Galactic SNRs. By measuring shape and level of the high-energy γ -ray emission the GLAST-LAT might allow for a distinction between hadronic and leptonic emission models as discussed in section 5. Other potential shell-type SNR counterparts related to this analysis are W 28 (HESS J1801–233 and 3EG J1800–2338), IC443/MAGIC J0616+225 (Albert et al. 2007b), and the Monoceros Loop SNR (HESS J0632+058 and 3EG J0634+0521) (Aharonian et al. 2007e), although in particular in the latter case, the morphology of the VHE γ -ray source does not lend support to an association with the SNR shell.

3.1.3. *γ -ray binaries*

Three binary systems: PSR B1259–63/SS 2883, LS 5039 and LSI+61 303, have now been established as VHE γ -ray sources (Aharonian et al. 2005c, 2006d; Albert et al. 2006; Smith et al. 2007). The latter two of these objects have long been considered as likely coun-

terparts to EGRET sources (Kniffen et al. 1997; Tavani et al. 1998; Hartman et al. 1999; Paredes et al. 2000), however, a definitive identification could not be achieved in the GeV waveband so far. The VHE γ -ray emission is undoubtedly related to the binary system (as e.g. in LS 5039 established through the detection of characteristic periodicity, matching the orbital period of the binary system), strengthening the case that the GeV emission is also associated to these binaries. Recently, the MAGIC collaboration presented evidence for VHE γ -ray emission from the black-hole X-ray binary Cyg X-1, during a flaring state in X-rays (Albert et al. 2007d). There is no evidence so far for GeV emission from this object.

3.2. Spectral compatibility

As described in section 2.2, a test for compatibility between EGRET and H.E.S.S. energy spectra based on a single power-law extrapolation has been performed, calculating for each of the coincident cases in the H.E.S.S. GPS region a measure of spectral mismatch: σ_{comb} . Figure 4 shows the result of these extrapolations. The values for the spectral compatibility parameter σ_{comb} are rather small. The largest value, potentially indicative of a spectral mismatch, is found for the case of the γ -ray binary association LS 5039 (3EG J1824–1514 and HESS J1826–148). However, this value is completely dominated by the small statistical error on the H.E.S.S. power-law fit below 1 TeV (error on the photon index: $\Delta\Gamma_{\text{stat}} = \pm 0.04$). Taking a typical H.E.S.S. systematic error of $\Delta\Gamma_{\text{sys}} = \pm 0.2$ on the determination of the photon index Γ into account, the GeV and TeV energy spectra in this source match well. Figure 4 therefore suggests that the energy spectra of sources that show a spatial association can generally be rather well described by a single power-law description across the entire energy range from 0.1 GeV to 1 TeV.

To estimate the chance coincidence of a spectral consistency the spectra of all 17 EGRET sources and of all 22 H.E.S.S. sources in the H.E.S.S. GPS region have been interchanged and “connected” to each other (i.e. the spectral compatibility of each H.E.S.S. source has been determined for each EGRET source – regardless of positional coincidence). The resulting distribution of σ_{comb} can be interpreted as the probability density function for σ_{comb} for randomly selected H.E.S.S. and EGRET sources and is shown in Figure 5 as a red histogram. This distribution should be compared to the measured distribution of σ_{comb} for positionally coincident pairs (black histogram). Even though the distribution for the scrambled sources shows a tail to large values of σ_{comb} , most random pairings result in values of $\sigma_{\text{comb}} < 5$. A Kolmogorov test yields a probability of 89% that the two distributions are based on a common underlying distribution. Thus a spectral compatibility based on a power-law extrapolation of a typical (randomly picked) EGRET and a typical H.E.S.S. source is expected to occur by

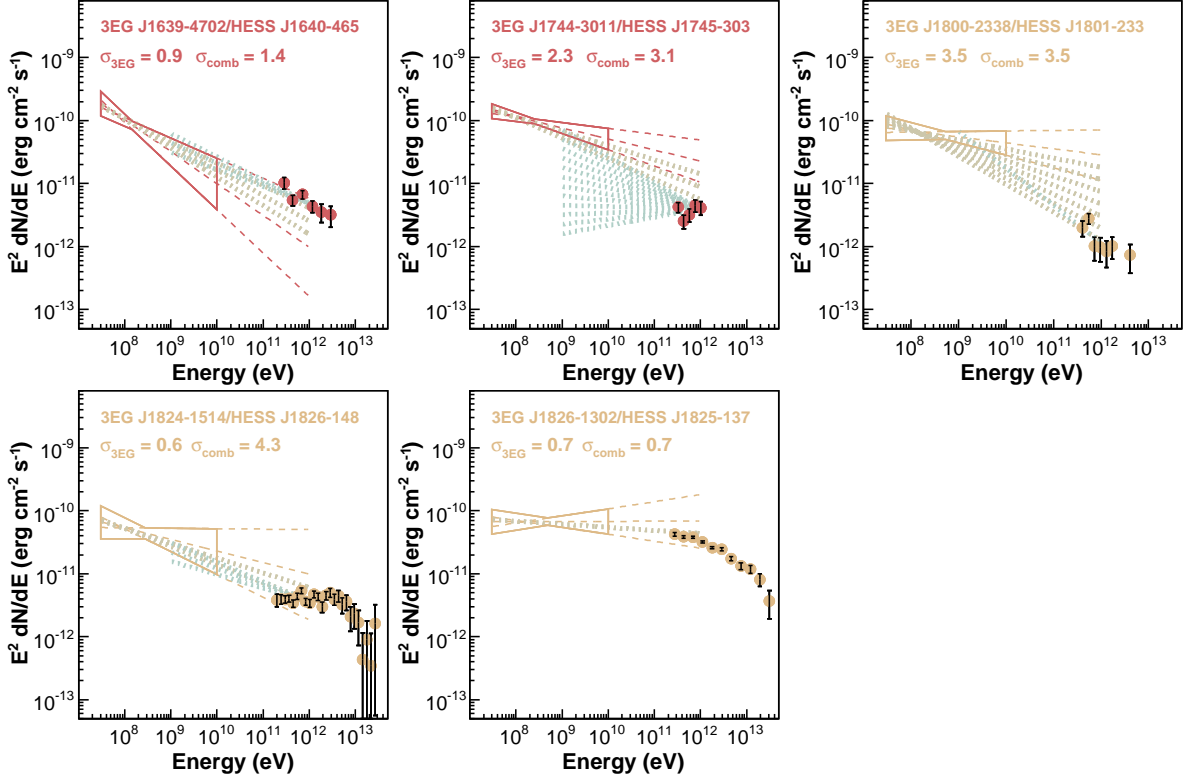


Fig. 4.— Spectra for the positionally coincident EGRET and H.E.S.S. sources within the H.E.S.S. GPS region. Sources for which the H.E.S.S. source is located within the 95% confidence level are shown in red, whereas those within the 99% confidence contour (as give in Table 1) are shown in orange. The EGRET “butterfly” is determined from the 3EG catalogue (Hartman et al. 1999), the H.E.S.S. spectral points are taken from the respective publication. For HESS J1826–148 and HESS J1825–137, which have significantly curved TeV spectra, only the spectral points below 1 TeV have been fitted and used for the extrapolation. Large values of σ_{comb} indicate mismatches between the spectra at GeV and at TeV energies.

chance even in the absence of a physical association. This is perhaps not surprising, given that both EGRET as and H.E.S.S. spectra have typical photon indices of ~ 2.3 and that H.E.S.S. measurements occur ~ 4 orders of magnitude higher in energy with H.E.S.S. being 1–2 orders of magnitude more sensitive.

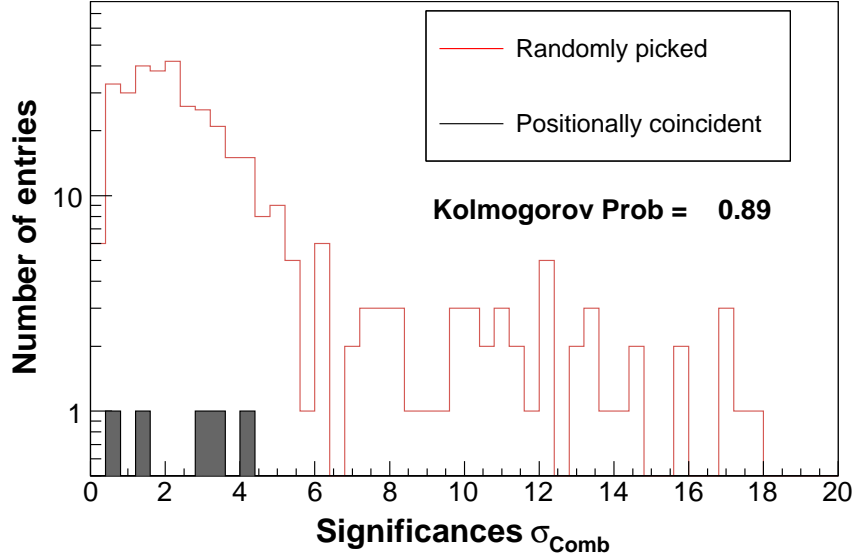


Fig. 5.— Distribution of σ_{comb} . The red histogram shows the distribution for the spectral consistency parameter σ_{comb} of all possible combinations of EGRET sources with H.E.S.S. sources within the GPS region. The black histogram shows the same distribution for the 5 cases of positional coincidences.

4. Inner Galaxy γ -ray sources detected in only one band

In this section the remainder (and majority) of sources in the H.E.S.S. GPS region will be discussed. These are the sources which do not have a counterpart in the neighbouring energy band. In Section 4.1 EGRET sources without a VHE γ -ray counterpart will be discussed, section 4.2 investigates VHE γ -ray sources without an EGRET counterpart.

4.1. EGRET sources without a VHE γ -ray counterpart

Here those EGRET sources are addressed with a 99%-confidence centroid position region which does not contain a reported VHE γ -ray source centroid. This sample consist of 12 EGRET detections, with $E > 100$ MeV fluxes ranging between 0.4 and $3.1 \times 10^{-6} \text{ cm}^{-2} \text{ s}^{-1}$ and photon indices of the power-law fits between ~ 1.75 and 3.2 . For these 12 EGRET sources, 2σ upper limits on the VHE flux at 1 TeV for the nominal EGRET position were determined. This was done by scaling the H.E.S.S. sensitivity for a 5σ point source detection (1% of the Crab in 25 h under the assumption of a photon index of 2.6) to the actual exposures as published for the H.E.S.S. GPS region (Aharonian et al. 2006g). As

EGRET Source	H.E.S.S. Upper Limit (10^{-12} ergs cm $^{-2}$ s $^{-1}$)	σ_{comb}
3EG J1655-4554	0.4	1.3
3EG J1710-4439	1.5	16.3
3EG J1714-3857	0.2	1.5
3EG J1718-3313	1.0	0
3EG J1734-3232	0.6	1.4
3EG J1736-2908	0.3	3.5
3EG J1746-2851	0.2	15.7
3EG J1809-2328	0.5	6.4
3EG J1812-1316	2.1	1.0
3EG J1823-1314	0.4	0
3EG J1837-0423	0.6	0
3EG J1837-0606	0.4	5.5

Table 3: EGRET sources without a VHE γ -ray counterpart in the H.E.S.S. GPS region. The H.E.S.S. differential upper limits (2σ) at 1 TeV for a point-source analysis, are derived from the H.E.S.S. 2004–2005 exposure at the nominal EGRET position as described in the text (under the assumption of a photon index of 2.6).

described previously, the spectral compatibility parameter $\sigma_{3\text{EG}}$ was determined according to Equation 2. For cases in which the EGRET extrapolation with the nominal 3EG photon index undershoots the H.E.S.S. upper limit, $\sigma_{3\text{EG}}$ is set to zero. The resulting plots are shown in Figure 6. For Gaussian errors $\sigma_{3\text{EG}}$ represents the probability that the true GeV spectrum would pass through the HESS upper limit.

In seven of the twelve cases the H.E.S.S. upper limit does not impose a strong constraint on an extrapolation of the EGRET spectrum ($\sigma_{3\text{EG}} < 1.5$). For the remaining five sources a H.E.S.S. detection would have been expected, based on a naïve power-law extrapolation. In particular extrapolations for four of the EGRET sources exhibiting a hard energy spectrum (3EG J1710–4439, 3EG J1746–2851, 3EG J1809–2328, and 3EG J1837–0606) are incompatible with the H.E.S.S. upper limits at levels exceeding $\sigma_{3\text{EG}} > 5$. For these cases the VHE γ -ray data strongly suggest a spectral turnover (cutoff or break) well below the H.E.S.S. range. Such behaviour is not surprising for some Galactic source classes. For the EGRET-detected pulsars a cutoff in the energy spectrum is seen in many sources *within* the EGRET energy regime (and therefore clearly well below the VHE range). Indeed, for three out of the four EGRET sources for which a spectral change is implied by the H.E.S.S.

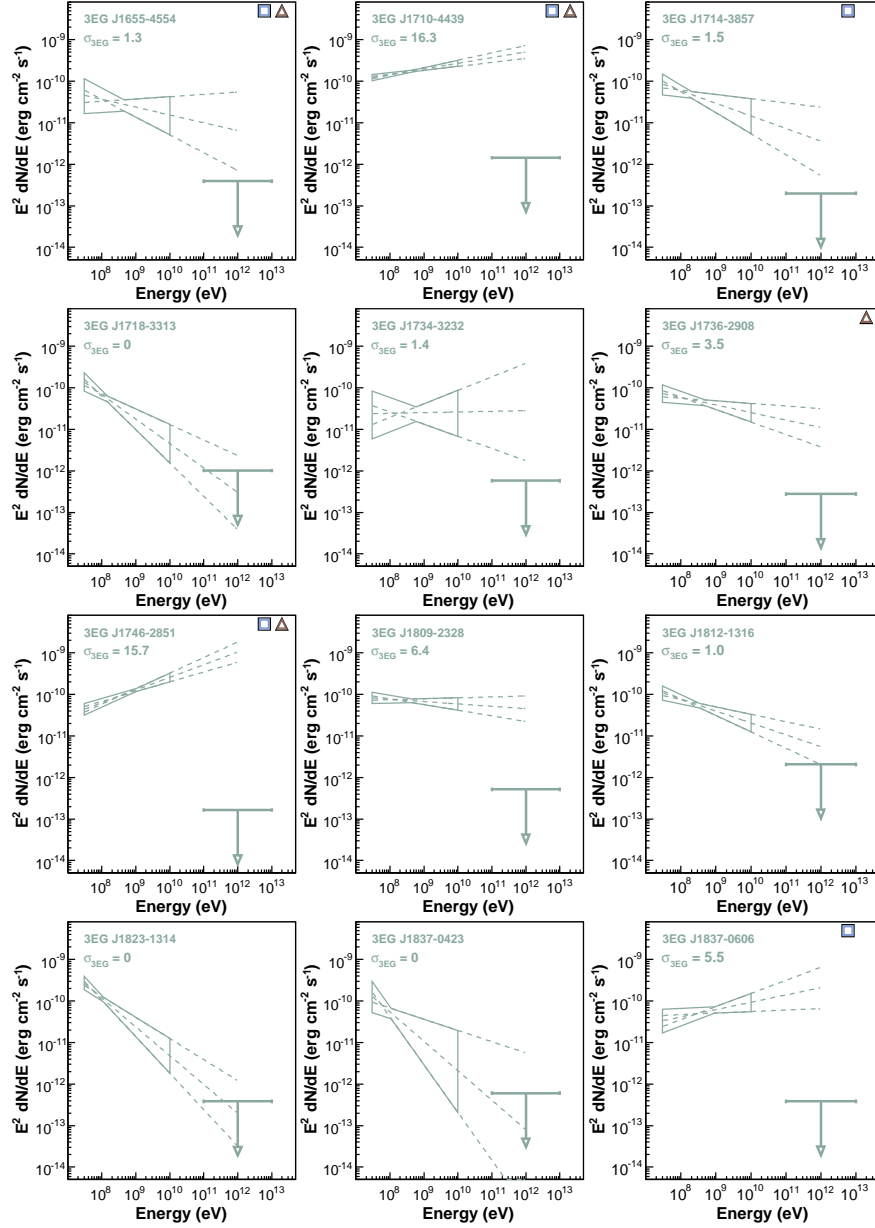


Fig. 6.— SED of the EGRET source for which no VHE γ -ray source was found within the 99% confidence contour. Sources marked with a square show γ -ray emission above 10 GeV in the EGRET data as reported by Thompson, Bertsch & O’Neal (2005), for sources marked with a triangle the EGRET data are better described by either a broken power-law or a power-law with an exponential cutoff as shown in Figure 7.

non-detection, a pulsar association has been proposed: 3EG J1710–4439 was unambiguously identified with PSR 1706–44 (Thompson et al. 1994), 3EG J1809–2328 was proposed to be of PWN nature (Braje et al. 2000), and 3EG J1837–0606 was suggested as the counterpart of PSR J1837–0604 (D’Amico et al. 2001). The remaining source in the sample for which the spectral extrapolation of the EGRET source is constrained by the H.E.S.S. upper limit, is the Galactic Centre source 3EG J1746–2851. This object is extremely interesting and important, and may be related to the TeV emission detected in this region, however, a proper discussion falls beyond the scope of this paper.

It is interesting to note that an analysis of the EGRET data above 10 GeV (Thompson, Bertsch & O’Neill 2005) found eleven EGRET sources with evidence for emission above 10 GeV (at a level of less than 10% probability that the number of photons seen is a fluctuation of the diffuse background emission). Five of these sources are located in the H.E.S.S. GPS region. These sources are 3EG J1655–4554, 3EG 1710–4439 (PSR B1706–44, with a 6.1σ detection significance above 10 GeV) 3EG J1714–3857, 3EG J1746–2851, and 3EG J1837–0606 (all marked with a white-and-blue square in Figure 6). Interestingly, all of these sources belong to the class of non-coincident sources, i.e. have no counterpart at VHE γ -ray energies. The characteristic cut-off energies of these sources are therefore likely confined to the region below ~ 100 GeV. This emphatically emphasises the existence of cutoffs within the energetic gap left between the end of the EGRET measurements and the onset of the H.E.S.S. and MAGIC observations.

To further investigate the cutoff hypothesis a spectral analysis of the EGRET energy spectra has been performed by means of higher order representations, as has been reported by Bertsch et al. (2000); Reimer & Bertsch (2001). The EGRET spectra were fitted with a broken power-law and with a power-law with an exponential cutoff:

$$\frac{\partial J}{\partial E}(E, K, \lambda_1, \lambda_2) = \begin{cases} K \left(\frac{E}{1\text{GeV}}\right)^{-\lambda_1} & (E \leq 1\text{GeV}) \\ K \left(\frac{E}{1\text{GeV}}\right)^{-\lambda_2} & (E \geq 1\text{GeV}) \end{cases} \quad (3)$$

$$\frac{\partial J}{\partial E}(E, K, \lambda, E_c) = K \left(\frac{E}{300\text{MeV}}\right)^{-\lambda} \exp\left(-\frac{E}{E_c}\right) \quad (4)$$

The χ^2 of the resulting fits were compared to that for a single power-law and an F-test employed to test if the more complex form was justified. For many γ -ray sources there is insufficient high-energy data to justify higher order functional fits. However, for four of the 17 EGRET sources considered in this study the F-test strongly suggests a different spectral form (with a chance probability < 0.05 as discussed in detail in Reimer & Bertsch (2001)): 3EG J1655–4554 is better fit by a power-law with exponential cutoff, 3EG J1710–

4439, 3EG J1736-2908, and 3EG J1746-2851 are best fit with a broken power-law. All of these sources have no positional counterpart at TeV energies (and are marked with triangles in Figure 6). The different spectral representations are shown in red in Figure 7. It is interesting to note, that out of the four sources mentioned above for which the H.E.S.S. non-detection strongly suggests a cutoff in the energy spectrum, the two sources with the largest incompatibility measure $\sigma_{3\text{EG}}$ are also characterised by a statistically significant cutoff in the EGRET spectrum. In particular, the previously mentioned source 3EG J1746-2851 (Galactic Centre) shows strong indications for an energy break below 10 GeV. The indicated cutoff in some of the EGRET spectra is entirely consistent with the constraining VHE limit based on power-law extrapolation. The prediction that the other two EGRET sources (3EG J1809-2328, and 3EG J1837-0606) constrained by the H.E.S.S. upper limits show a cutoff in the energy range between 10 GeV and 100 GeV is therefore well justified and will be tested by upcoming GLAST-LAT observations.

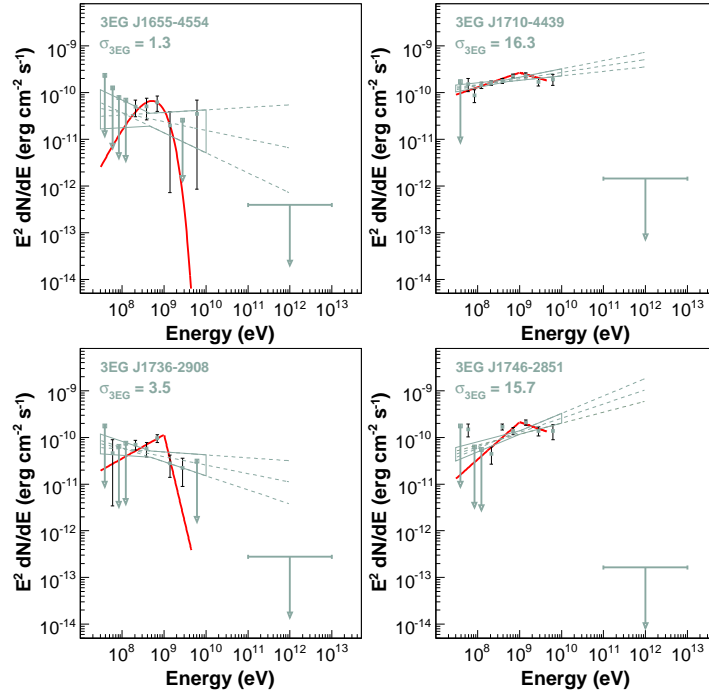


Fig. 7.— SED at $E > 30$ MeV for the non-coincident cases in which the EGRET spectrum shows significant deviation from a simple power-law form. The previously reported higher order spectral representations are shown in red (exponential cutoff for 3EG J1655-4554 and broken power-law for 3EG J1710-4439, 3EG J1736-2908 and 3EG J1746-2851).

4.2. VHE γ -ray sources without an EGRET counterpart

In this section the H.E.S.S. sources without a catalogued EGRET counterpart are addressed. At all nominal H.E.S.S. source locations, flux upper limits have been determined from the EGRET data at energies above 1 GeV by means of the EGRET likelihood technique (Mattox et al. 1996). In the determination of the EGRET upper limit, both the Galactic diffuse emission and point-sources exceeding a 5σ -detection significance threshold were modelled and subsequently subtracted. The underlying EGRET exposure corresponds to the first four years of the EGRET mission. As previously discussed, the sensitivity of EGRET (in terms of energy flux $E^2 dN/dE$) is considerably worse than the H.E.S.S. sensitivity so that no EGRET detection of a H.E.S.S. source is expected under the assumption of equal energy flux – which might obviously not necessarily be fulfilled in an astrophysical source.

Methodologically similar to the previous section, the determination of spectral compatibility was performed by extrapolating H.E.S.S.-measured VHE spectra to 1 GeV and comparing the resulting flux to the EGRET upper limit at that energy. The spectral compatibility parameter $\sigma_{\text{H.E.S.S.}}$ is determined in a similar way to $\sigma_{3\text{EG}}$. The spectra of H.E.S.S. sources with significant curvature were only fitted from the threshold energy at ~ 100 GeV to 1 TeV. As in previous sections, $\sigma_{\text{HESS-EGRET}}$ describes how well the extrapolated H.E.S.S. spectrum can be accommodated by the EGRET upper limit. The resulting spectral energy distributions (SEDs) of the non-coincident H.E.S.S. sources are shown in Figures 8 and 9.

In all cases, the values of $\sigma_{\text{HESS-EGRET}}$ are less than or equal to 1, implying that no EGRET upper limit is violated by the H.E.S.S. extrapolation to 1 GeV, in stark contrast to the results discussed in the previous section. The most interesting case is that of HESS J1713–395 (RX J1713.7–3946). In this case the power-law extrapolation is at the level of the EGRET upper limit and $\sigma_{\text{HESS-EGRET}} = 1$. The unconstraining nature of the EGRET upper limits is simply a consequence of a lack of instrumental sensitivity at GeV energies, worsened in regions of pronounced diffuse γ -ray emission such as the H.E.S.S. GPS region. However, this situation will change significantly in the near future, given the expected sensitivity of the GLAST-LAT as also shown in Figures 8 and 9 in which $\sigma_{\text{HESS-GLAST}}$ is calculated for a typical one-year GLAST sensitivity limit in the Inner Galaxy. These numbers suggest that the increased sensitivity of the LAT might render common GeV-TeV studies possible. While the EGRET upper limits are currently insensitive to linear extrapolations of the H.E.S.S. spectra, the GLAST-LAT will clearly allow for more sensitive studies. It should, however, be noted, that a linear extrapolation between H.E.S.S. and GLAST-LAT energies most probably represents the “best-case” for any such study: physical models typically show spectra that harden towards GeV energies, unless a different emission component/process takes over. It

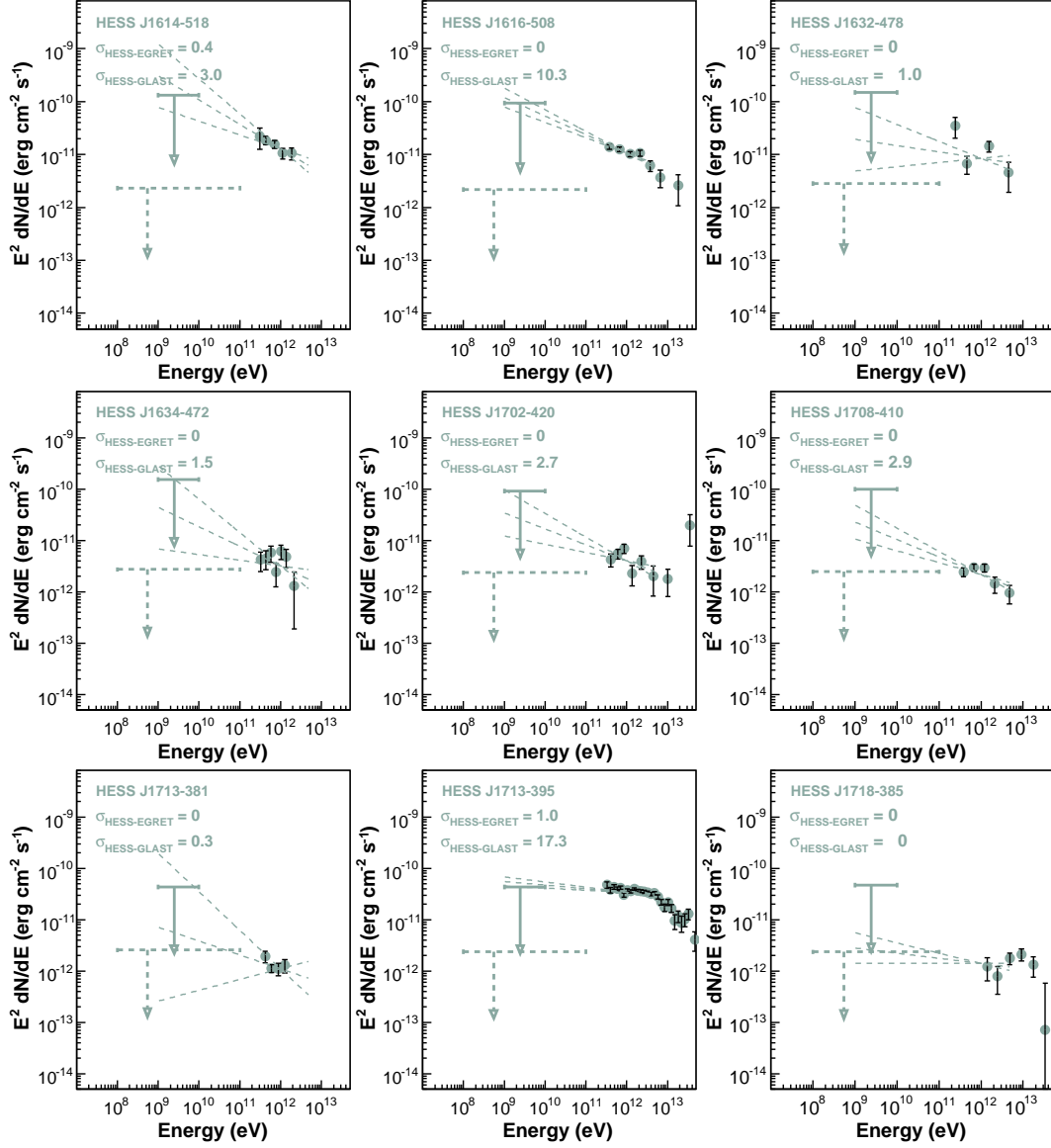


Fig. 8.— (Part 1) SED at $E > 30$ MeV for the cases in which no EGRET catalogued counterpart source was found for the H.E.S.S. source. The dashed arrow shows the predicted upper limit from a one-year GLAST scanning observation, taking into account the galactic diffuse background. Derived from this is the spectral compatibility parameter $\sigma_{\text{HESS-GLAST}}$ between GLAST and H.E.S.S. assuming a non-detection with GLAST to illustrate that GLAST will be able to probe the power-law extrapolation from VHE γ -ray energies whereas the existing EGRET upper limits are unconstraining in this regard.

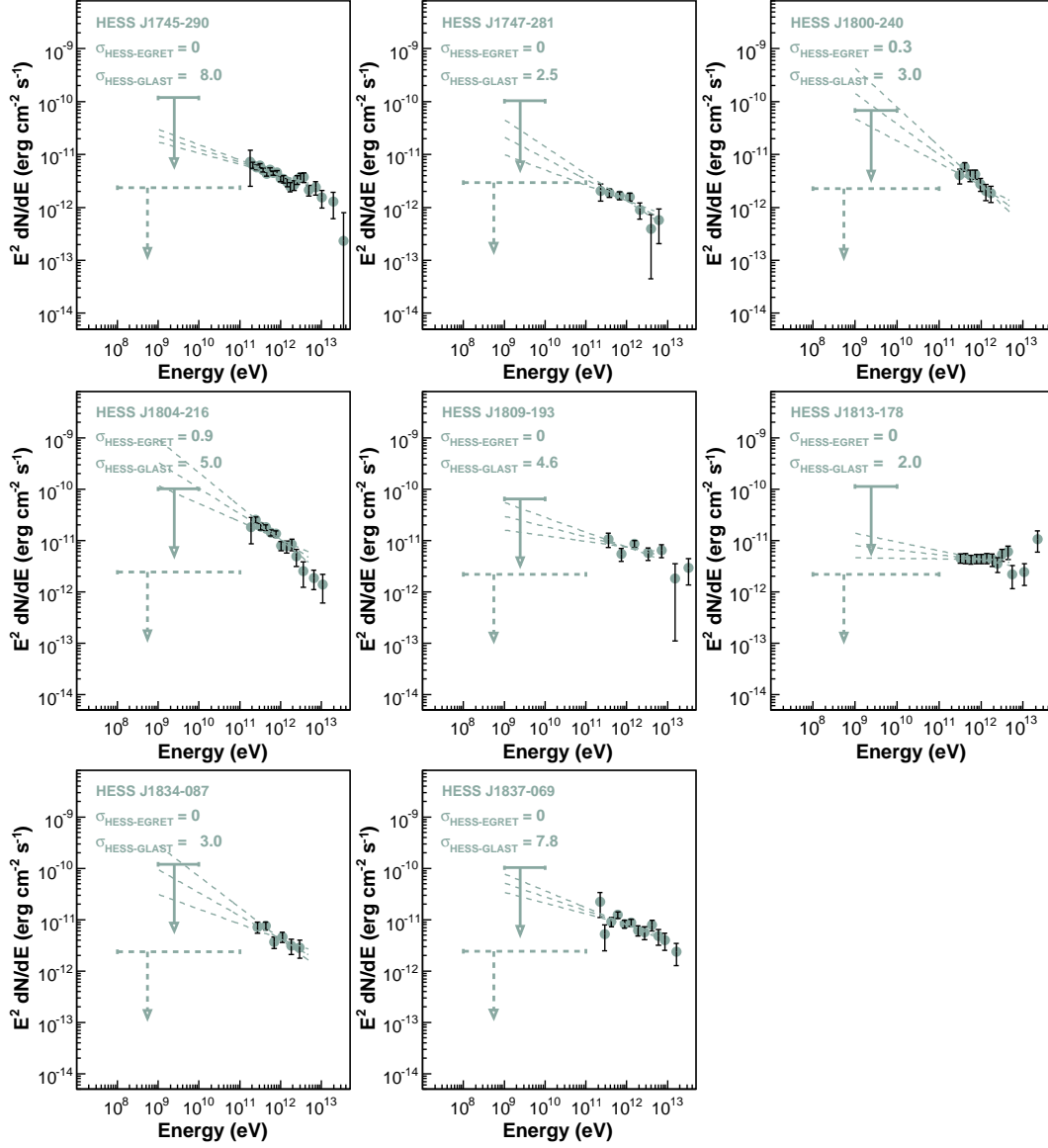


Fig. 9.— (Part 2) SED at $E > 30$ MeV for the cases in which no EGRET catalogued counterpart source was found for the H.E.S.S. sources. The dashed arrow shows the predicted upper limit from a one-year GLAST scanning observation, taking into account the diffuse emission. Derived from this is the spectral mismatch between GLAST and H.E.S.S. assuming a non-detection with GLAST to illustrate the GLAST will be able to probe the power-law extrapolation from VHE γ -ray energies whereas the EGRET upper limits are unconstraining in this regard.

remains to be seen if GLAST will detect emission at comparable energy flux and potentially determine the position of the peak in the SEDs. As discussed previously, the tremendous advantage of the GLAST-LAT over any previous mission is the continuous energy coverage from 30 MeV all the way up into the VHE γ -ray range at ~ 300 GeV with significantly improved sensitivity and angular resolution, bridging the current energy gap in which some of the physically interesting suggested energy cutoffs occur.

5. Interpretation

5.1. Sources detected both at GeV and TeV energies

As previously stated and shown in Table 2, only 9 sources exist which can be characterised as coincident Galactic EGRET and VHE γ -ray sources at this moment (5 within the inner Galaxy, 4 outside of the H.E.S.S. GPS region). Given the large number of Galactic sources in both GeV and TeV γ -rays this number is rather small – and is indicative of different dominant source classes in these two energy domains. However, for the few cases where a positional coincidence may exist some important astrophysical implications as well as predictions for the upcoming GLAST mission can be drawn.

Whilst EGRET and in particular GLAST have sufficiently large FoVs to be able to efficiently observe the whole sky, the limited FoV of imaging VHE γ -ray instruments (typically 4° diameter) allow for only limited sky coverage. However, for known GeV sources high-angular resolution VHE instruments such as MAGIC and H.E.S.S. with tremendously higher photon statistics at high energies can help in the identification and interpretation of the GeV emission. This approach has been followed by Reimer & Funk (2007) for the Kookaburra complex. In this region of TeV and GeV γ -ray emission, a re-analysis of the EGRET data taking advantage of the higher spatial resolution images from H.E.S.S. observations, demonstrated that the dominant GeV emission (3EG J1420–6038) is positionally coincident with HESS J1420–607 (Aharonian et al. 2006c). This EGRET source has been flagged as confused in the 3EG catalogue (Hartman et al. 1999) and in the re-analysis 3EG J1420–6038 was found to be partially overlapping with a less intense second GeV γ -ray source. This second GeV source – detected below the nominal detection threshold for EGRET – is apparent in a dedicated analysis at approximately 1/3 of the GeV flux of the dominant source (Reimer & Funk 2007) and is positionally coincident with the second VHE γ -ray source in the Kookaburra region, HESS J1418–609 (Aharonian et al. 2006c) (associated with the “Rabbit” PWN). This suggestive morphology match between the GeV data and the H.E.S.S. data thus helped in the interpretation and identification of the confused EGRET sources and made a separation into two individual sources possible. Studies such as this one

show how confused GeV emission regions (in particular in the Galactic plane where the diffuse γ -ray background is dominant) may be unravelled using the GeV emission as measured from a large-aperture space-based γ -ray instrument together with narrow FoV but superior spatial resolution observations provided by ground-based atmospheric Cherenkov telescopes. This approach seems promising for achieving convincing individual source identifications in the era of the GLAST-LAT.

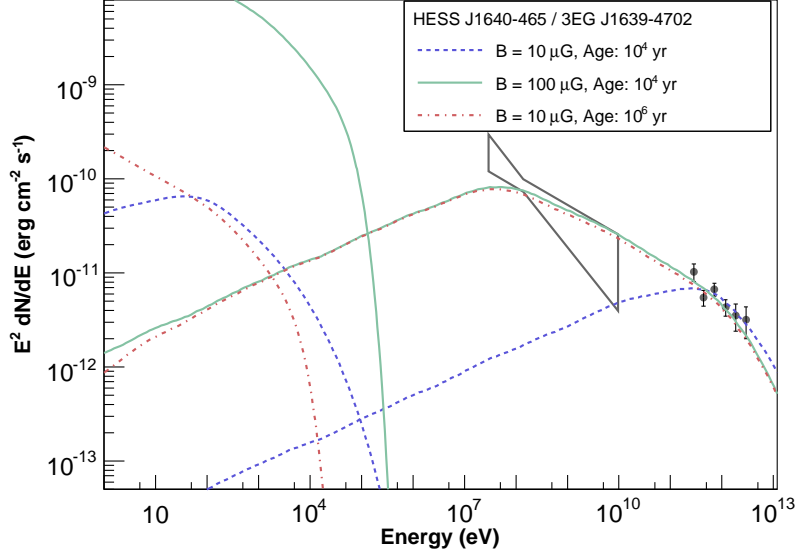


Fig. 10.— SED for the coincident source HESS J1640-465 along with leptonic IC-models for different magnetic fields and different ages of the system. The purpose of this figure is to demonstrate that rather extreme values for the magnetic-field ($\sim 100\mu\text{G}$) or the age of the system ($\sim 10^6$ years) have to be invoked to fit such a spectral energy distribution in a leptonic model. These models numerically take into account the time-evolution of the electron spectrum considering energy losses and injection of electrons in time-steps much shorter than the age of the system. Synchrotron and IC losses are calculated following the formalism in Blumenthal & Gould (1970). The injection spectrum for the electrons was chosen to have a photon index of 2.5, the Inverse Compton scattering was performed on the CMB only. It should be noted, that the X-ray flux between 2 and 10 keV detected from this source is at the level of $10^{-13} \text{ erg cm}^{-2} \text{ s}^{-1}$ as determined by Funk et al. (2007). This rather low X-ray flux renders a connection between the H.E.S.S. and the EGRET source in any leptonic model extremely difficult as demonstrated by this figure.

On the other hand, the detection of VHE γ -ray sources with EGRET (or the GLAST-LAT) may help in the interpretation of the TeV data and the modelling of the γ -ray emission

mechanism. Measuring the energy spectrum of a high-energy γ -ray source over 5–6 decades in energy should provide rather stringent constraints on the γ -ray emission mechanism. The Crab is in this respect the only good example of a Galactic source for which both an excellent GeV and TeV coverage exists which in turn helped to understand the emission mechanism and the magnetic field strength rather well in comparison to most other γ -ray sources. With the advent of the GLAST-LAT many more such sources with a good GeV and TeV coverage can be expected.

Figure 10 shows the SED for the positionally coincident sources 3EG J1639–4702 and HESS J1640–465 (Aharonian et al. 2006g; Funk et al. 2007). The figure shows a rather typical γ -ray SED for a positionally coincident sources (see Figure 4) with a power-law spectrum at TeV energies with photon index 2.4 ± 0.15 and a similar power-law at GeV energies with photon index 2.5 ± 0.18 , at an energy flux level an order of magnitude higher than that at 1 TeV. The EGRET source 3EG J1639–4702 is rather close to the detection significance threshold (with a $TS^{1/2}$ -value of 6.4). Taking this SED as representative, several scenarios for a common origin of the γ -ray emission are considered. For a hadronic model the shape of this SED can be rather easily fitted, requiring a power-law distribution of primary hadrons with $dN/dE \propto E^{-\alpha}$, with $\alpha \approx 2.5$ and a maximum particle energy beyond the TeV range. However, for a simple leptonic model, with the γ -ray emission interpreted as inverse-Compton up-scattering of soft photon fields, matching the shape of the SED requires rather extreme values for the magnetic field (given the low level of X-ray synchrotron emission from this system as reported by Funk et al. 2007) or for the age of the system (given the need to confine the accelerated electrons within the system). This is demonstrated in Figure 10 which shows 3 leptonic model curves. In the generation of these models, the time-evolution of the electron spectrum due to energy losses was taken into account. These energy losses were calculated according to the formalism described in Blumenthal & Gould (1970). For high energy electrons the energy-loss (cooling) timescale $E/(dE/dt)$ is proportional to $1/E$ for losses predominantly via synchrotron radiation or IC in the Thomson regime. In this case, for continuous injection of electrons with a power law spectrum $dN/dE \propto E^{-\alpha}$, a spectral break to $E^{-(\alpha+1)}$ will occur. The slope of the IC spectrum (again in the Thomson regime) is given by $\Gamma = (\alpha + 1)/2$. In the idealised case of the Thomson cross-section and a single (thermal) target radiation field the break energy is given approximately by:

$$E_{\text{break}} \approx 0.4(t_{\text{source}}/10^6\text{yr})^{-2}((U_{\text{rad}} + B^2/8\pi)/1\text{eV cm}^{-3})^{-2}(T/2.7\text{ K})\text{ GeV} \quad (5)$$

In all cases shown in Figure 10, the time-independent injection spectrum of the electrons was fixed with an index of 2.5 and a cutoff energy at 100 TeV, with the IC scattering on the cosmic microwave background (CMB) alone. The first curve (dashed blue) is derived using values rather typically assumed for TeV sources: a magnetic field strength $10\mu\text{G}$ and age of 10^4 years. This curve provides an adequate description of the H.E.S.S. data, but not

the EGRET data due to the characteristic turnover of the γ -ray spectrum at lower energies. The other two curves (solid green and dash-dotted red) are shown to illustrate how the SED could be accommodated in a leptonic model and thus how the peak of the IC emission can be pushed into the EGRET range. Taking a typical Galactic radiation field (which might not be realistic as e.g. in binary system with a massive stellar component) either rather high magnetic fields (green solid) or rather old sources have to be invoked (dash-dotted red). The high-magnetic field scenario would, however, lead to the prediction of a very high X-ray flux. This prediction contradicts the faint X-ray emission detected from this object (at the level of 10^{-13} erg cm $^{-2}$ s $^{-1}$) as well as in most other Galactic VHE γ -ray sources (where the X-ray emission is typically at the same level or below the VHE γ -ray energy flux). To explain the γ -ray emission of coincident sources through leptonic IC emission, the sources should thus be rather old to be able to accumulate enough low energy electrons to explain the high GeV flux in a typical Galactic radiation field. They should then, however, either be rather bright X-ray emitters or be very old.

VHE γ -ray sources may be detectable using GLAST even if the γ -ray emission is generated by IC scattering on a typical Galactic radiation field, as demonstrated for the SNR RX J1713.7–3946 where a GLAST detection should shed light on the heavily debated origin of the TeV emission (Funk et al. 2007b). γ -rays of leptonic origin (produced by IC) might be distinguishable from those of hadronic origin (produced by π^0 -decay) through their characteristic spectral shape, although recent claims have been made that under certain conditions the leptonic γ -ray spectra might resemble those of pionic decays (Ellison et al. 2007). Figure 11 shows that the GLAST-LAT will have the sensitivity to measure energy spectra (in 5 years of scanning observations) for both hadronic and leptonic emission scenarios, illustrating that the LAT energy range is particularly well suited to distinguish these models. Measuring the spectral shape of the γ -ray emission through deep GeV observations with the GLAST-LAT will play an important role in interpreting the currently known TeV γ -ray sources.

5.2. The non-connection of GeV and TeV sources

For sources where no positional coincidence has been found for the GeV and TeV domains both instrumental and astrophysical explanations can be invoked.

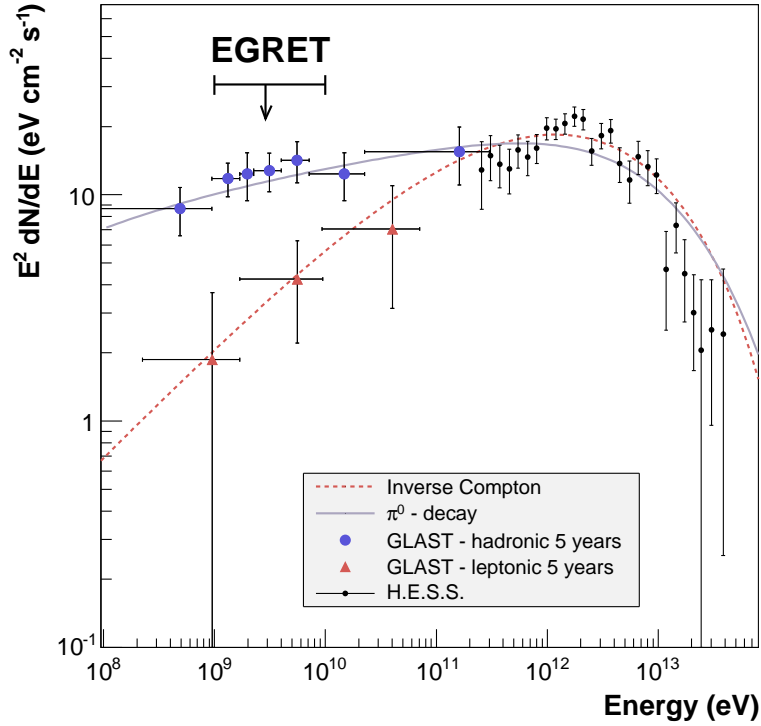


Fig. 11.— High-energy SED for the SNR RX J1713.7–3946. The black data points show measurements with H.E.S.S., whereas the blue circles and red triangles show simulated GLAST data, assuming two different models (leptonic and hadronic) for the γ -ray emission (shown as dashed red and solid blue lines). This simulation uses the current best estimate of the LAT performance and illustrate that in principle the GLAST-LAT should be able to detect this prominent shell-type SNR in a 5-years observation or faster, depending on the emission mechanism. This figure has been reproduced from (Funk et al. 2007b).

5.2.1. Instrumental reasons for non-connection

The most obvious reason for a non-detection of a TeV source with EGRET is the sensitivity mismatch. In a typical ~ 5 hour observation H.E.S.S. has an energy flux sensitivity of about a factor of $\sim 50 - 80$ lower than that of EGRET for its entire lifetime (above 1 GeV in the Galactic Plane). Additionally, with decreasing detection significance an increasing number of EGRET sources are expected to be artificial due to source confusion in the Galactic plane and in particular due to uncertainties from the model chosen to describe the dominant diffuse γ -ray emission. The GLAST-LAT will inevitably shed more light on all persistent EGRET sources, since these will be rather bright γ -ray sources for the LAT

instrument. However, it should be noted that the brightest Galactic H.E.S.S. sources (such as RX J1713.7–3946) are not going to be very bright GLAST sources as discussed in the previous section. Certainly, similar to EGRET, the LAT will (at the lower end of the energy range) suffer from uncertainties and systematic effects due to intrinsic properties of the experimental approach and in particular due to the modelling of the diffuse γ -ray background, however, at a lower flux level.

Another instrumental effect that could render a correlation between GeV and TeV sources unlikely, is the insensitivity of imaging VHE γ -ray instruments to very extended sources (radius $> 1^\circ$) without significant sub-structure. The EGRET data do not put strong constraints on the source extension of a typical source in the Galactic plane. Source extensions that can be derived from the data are on the scale of the EGRET PSF, i.e. degree scales. The angular resolution (and thus the maximum sensitivity) of VHE γ -ray instruments on the other hand is of the order of a few arc minutes. The upper limits for H.E.S.S. at the positions of EGRET sources quoted in this study are derived under the assumption of a point-like source (with a typical size of the source region of less than $\sim 0.1^\circ$ rms width). The sensitivity and thus the upper limit scales roughly linearly with the source size (Funk 2005) and for source sizes in excess of $\sim 1^\circ$, the H.E.S.S. data become completely unconstraining due to the fact that the source size becomes comparable with the size of the FoV and no reliable background estimation can be performed (see Berge, Funk & Hinton 2007, for a description of the background estimation techniques used). Large-FoV instruments (with poorer angular resolution) such as Milagro (Atkins et al. 2002), are better suited to detect sources with intrinsically large sizes in VHE γ -rays (with sufficiently high fluxes). However, due to their modest ($\sim 1^\circ$) angular resolution, such instruments suffer from problems of source confusion similar to those of current GeV measurements. Indeed, several of the recently reported Milagro source candidates are coincident with EGRET sources (Abdo et al. 2007). Hypothesising that EGRET sources exhibit angular sizes larger than $\sim 1^\circ$, Milagro-type instruments might be better suited to detect large scale emission at VHE γ -ray energies. Again, the GLAST-LAT, with its superior angular resolution to EGRET, will shed more light on the issue of the intrinsic sizes of GeV sources in the Galactic plane. The constraints on the power-law extrapolation of EGRET sources by sensitive H.E.S.S. upper limits as derived in the previous sections are naturally only valid under the assumption that the VHE counterpart to the EGRET emission does not exhibit a size much larger than $\sim 1^\circ$.

5.2.2. Astrophysical reasons for non-connection

The non-detection of most TeV sources in the GeV range by EGRET may be due simply to a lack of instrumental sensitivity. On the other hand, the lack of TeV counterparts to most bright GeV sources requires the presence of steepening (or cut-offs) between 10 and 100 GeV in the spectra of these sources (see section 4 and Figure 7). Steepening in γ -ray energy spectra between 10 and 100 GeV can occur for many reasons, the most prominent of which are discussed briefly below.

Acceleration limits. The maximum energy to which particles are accelerated in a source may be determined by a balance between the acceleration and energy loss timescales, or between acceleration and escape timescales, or simply by the lifetime of the source. In the limit of Bohm diffusion, the escape time of accelerated particles from the source can be written as

$$t_{\text{escape}} \sim (r_{\text{source}}/\text{pc})^2 D_0 (E/\text{TeV})^{-\Delta} \quad (6)$$

The associated cut-off in the resulting γ -ray emission may occur at much lower energies, as in the case of proton-proton interactions (a factor ~ 20 as shown in Kappes et al. 2007), or close to the primary particle energy, as in the case of inverse Compton scattering in the Klein-Nishina limit (Blumenthal & Gould 1970).

Particle transport may impact on the spectral shape in several ways. For protons described by a power-law $J_p(E_p) = K E_p^{-\Gamma}$ the γ -rays produced in hadronic interactions are expected to follow a similar power-law spectrum $F_\gamma(E_\gamma) \propto E_\gamma^{-\Gamma}$. Generally, high energy particles escape more easily leading to a cut-off in the particle and hence γ -ray spectrum inside the source. Therefore, due to particle transport, the spectrum of the protons generating the γ -rays through hadronic interactions is not necessarily the same as the one at the acceleration site. In the case of diffusion the proton spectrum at the γ -ray production site can instead be written as $J_p(E_p, r, t) = \frac{c}{4\pi} f$, where $f(E_p, r, t)$ is the distribution function of protons at an instant t and distance r from the source. The distribution function satisfies the diffusion equation (Ginzburg & Syrovatskii 1964).

$$\frac{\partial f}{\partial t} = \frac{D(E_p)}{r^2} \frac{\partial}{\partial r} r^2 \frac{\partial f}{\partial r} + \frac{\partial}{\partial E_p} (P f) + Q, \quad (7)$$

where $P = -dE_p/dt$ is the continuous energy loss rate of the particles, $Q = Q(E_p, r, t)$ is the source function, and $D(E_p)$ is the diffusion coefficient. Atoyan, Aharonian & Völk (1995) derived a general solution for Equation (7). Hence, as has been emphasised by Aharonian & Atoyan (1996), the observed γ -ray flux can have a significantly different spectrum from that expected from the particle population at the source. In the (expected) case of energy-dependent diffusion ($D \propto E^{-\Delta}$, with Δ typically assumed to lie in the range $\sim 0.3 - 1.0$) the γ -ray spectrum

will follow $F_\gamma(E_\gamma) \propto E_\gamma^{-(\Gamma+\Delta)}$. The exact shape of the spectrum will depend on the age of the accelerator, duration of injection, the diffusion coefficient, and the location of the target material.

The influence of convection (lower energy cutoff in primary particle spectrum) is typically stronger for low energy (GeV) γ -rays potentially resulting in a VHE γ -ray source that has no EGRET counterpart in cases in which an external accelerator produces primary hadrons near an active target. Torres, Domingo-Santamaria & Romero (2004) and Domingo-Santamaria & Torres (2006) have recently studied collective wind configurations produced by a number of massive stars, and obtained densities and expansion velocities of the stellar wind gas that is the target for hadronic interactions in several examples, showing that these may be sources for GLAST and the TeV instruments in non-uniform ways, i.e., with or without the corresponding counterparts in the other energy band.

Particle energy losses away from the acceleration site may also produce spectral steepening in a very natural way as discussed earlier (see section 5.1). In the case where particle injection is effectively finished (i.e. the injection rate is much lower than in the past), radiative energy losses may produce a rather sharp cut-off in the γ -ray spectrum as e.g. shown in (Funk et al. 2007). For high energy electrons the energy-loss (cooling) timescale $E/(dE/dt)$ is proportional to $1/E$ for losses dominantly via synchrotron radiation or IC in the Thomson regime. In this case, for continuous injection of electrons with a power law spectrum $dN/dE \propto E^{-\alpha}$, a spectral break to $E^{-(\alpha+1)}$ will occur. The slope of the IC spectrum (again in the Thomson regime) is given by $\Gamma = (\alpha+1)/2$. In the idealised case of the Thomson cross-section and a single (thermal) target radiation field the break energy is given approximately by:

$$E_{\text{break}} \approx 0.4(t_{\text{source}}/10^6\text{yr})^{-2}((U_{\text{rad}} + B^2/8\pi)/1\text{eV cm}^{-3})^{-2}(T/2.7\text{K})\text{ GeV} \quad (8)$$

γ - γ *pair-production* occurs above a threshold $\epsilon_\gamma\epsilon_{\text{target}} > 2m_e^2c^4$. For stellar systems with $\epsilon_{\text{target}} \sim 1\text{ eV}$, this process occurs above $\sim 500\text{ GeV}$. Pairs produced in γ - γ interactions may inverse Compton scatter on the same radiation field – leading to the development of a cascade (Protheroe, Mastichiadis & Dermer 1992). Attenuation on the interstellar IR and CMB can be neglected below 10 TeV so γ - γ ‘cut-offs’ are only expected in compact regions of very high radiation density, for example within binary stellar systems. These absorption/cascade ‘features’ may not represent the end of the γ -ray spectrum as emission may recover at energies above the resonance.

5.3. Prospects for the GLAST-LAT

As demonstrated by Figures 8 and 9 the GLAST-LAT should be able to detect several of the VHE γ -ray sources in the inner Galaxy, assuming a simple power-law extrapolation of the spectrum from TeV to GeV energies. However, this power-law assumption may not be valid in several cases, as discussed in the following for the known TeV source classes.

Pulsar Wind Nebulae are currently the most abundant VHE γ -ray sources in the Galactic plane. The most prominent example is the Crab Nebula (Weekes et al. 1989; Aharonian et al. 2004; Atkins et al. 2003; Aharonian et al. 2006f; Albert et al. 2007a). The SED expected of PWNe does not typically result in significant GeV fluxes: the Crab Nebula, detected throughout both energy bands, seems to be an exceptional case due to its very strong magnetic field and relative proximity (2 kpc). Most VHE γ -ray PWNe are expected to be dominated by IC emission for which the energy flux generally turns down at lower energies. The position of this inverse Compton peak determines detectability for both GeV and TeV instruments. Also the size and flux of the source also obviously affect the detectability with GLAST-LAT. In general the higher the energy of the inverse-Compton peak in these sources, the lower the chance will be to detect them with GLAST. If a large fraction of the GeV emission attributed to EGRET Galactic unidentified sources is related to pulsed magnetospheric emission from pulsars as opposed to emission from the extended wind nebula then a correlation between the H.E.S.S. and EGRET sources in the Inner Galaxy could be expected, given that the majority of the H.E.S.S. sources in this region seem to be PWNe associated with energetic pulsars (Carrigan et al. 2007). However, this expectation may not hold in general due to diversity of parameters like the beaming geometry or different conversion efficiency of the pulsar’s spin-down power into the Nebula and into γ -rays.

Shell-type Supernova remnants The two prominent and bright VHE γ -ray SNRs (RX J1713.7–3946 and RX J0852.0–4622) are not expected to be very bright GLAST-LAT sources. Nevertheless, they are probably amongst the more easily detectable TeV sources in the GLAST-LAT band. A detailed simulation of the expected signal from RX J1713.7–3946 shows that it might be detectable in one year of GLAST-LAT observations depending on the assumed TeV γ -ray emission mechanism as shown in the previous section. Morphological studies in GeV γ -rays will either have to struggle with moderate angular resolution at low energies or with low photon statistic at high energies. However, spectral studies will be immediately possible following a potential detection as shown in Figure 11 for RX J1713.7–3946. For RX J0852.0–4622 (Vela Junior) the situation is even further complicated by the close-by bright Vela Pulsar. While both of these prominent TeV-emitting objects are rather young (~ 2000 years), there is the potential of older SNRs acting as stronger GeV emitters (but rather faint TeV sources). In this case the GLAST-LAT might see a different population of

shell-type SNRs than VHE γ -ray instruments, namely older SNRs which have accumulated a large number of lower energy CRs, but for which the higher energy CRs (those that may give rise to the TeV emission) have already left the acceleration site. A common detection both with GLAST and VHE γ -ray instruments might require a hadronic origin of the γ -ray emission rather than an Inverse Compton (IC) origin due to the characteristic turn-over of the IC spectrum at lower energies.

Gamma-ray Binary systems host a variety of non-thermal phenomena. The TeV detected binaries: LS 5039 (Aharonian et al. 2006d), PSR B1259-63 (Aharonian et al. 2005c), LSI +61 303 (Albert et al. 2006) and Cyg X-1 (Albert et al. 2007d) are currently seen as candidates for detection at GeV energies. γ - γ absorption in binary systems may producing anti-correlation of the TeV to GeV radiation during the orbit of these systems. These orbital modulations are predicted in basically all models for these systems, irrespective of the assumptions of a pulsar or a black hole compact object or the process by which high-energy radiation is emitted (see e.g. Dermer & Böttcher 2007; Dubus 2006; Paredes, Bosch-Ramon & Romero 2006). Details in predicted light-curves and spectral evolution in time are however rather distinctive (Khangulyan, Aharonian & Bosch-Ramon 2007; Sierpowska-Bartosik & Torres 2007).

6. Summary

The main results of the study of the relationship between GeV and TeV sources are:

1. There are rather few spatially coincident GeV-TeV sources for the considered Galactic region.
2. Those few positional coincident GeV-TeV sources could occur by chance, the chance probability of detecting two coincident sources within the H.E.S.S. GPS region is $\sim 40\%$, thus no strong hint for a common GeV/TeV source population is detected.
3. Spectral compatibility (based on a power-law extrapolation) seems present for most of the positionally coincident sources, but again, this is expected to occur by chance (as described in the text) given the sensitivity mismatch and the different energy bands.
4. Dedicated H.E.S.S. limits at the position of the EGRET sources are constraining for a power-law extrapolation from the GeV to the TeV range for several of the EGRET sources, strongly suggesting cutoffs in the energy spectra of these EGRET sources in the unexplored region below 100 GeV. Power-law extrapolation of EGRET spectra seem to be ruled out for most of the EGRET sources investigated in this study.

5. Dedicated EGRET limits at the position of the H.E.S.S. sources are not constraining for a power-law extrapolation from the TeV to the GeV range. This picture will dramatically change once the GLAST-LAT with its improved sensitivity over EGRET is in orbit.
6. Several important mechanisms for cutoffs in the energy spectra of GeV sources have been discussed. There are well motivated physical reasons why the population of GeV and of TeV sources might be distinct.
7. If a source can be detected with both GeV and TeV instruments, the huge energy “lever arm” over 5-6 decades in energy will undoubtedly provide stringent constraints on the γ -ray emission mechanism in these Galactic particle accelerators.

Summarising, the study presented here shows that the GLAST-LAT will tremendously advance the study of the relationship between GeV and TeV sources by improving the sensitivity over EGRET by an order of magnitude and in particular by bridging the currently uncovered energy range between 10 GeV and 100 GeV.

The authors would like to acknowledge the support of their host institutions. In particular, S.F. acknowledges support of the Department of Energy (DOE) and Stanford University and would like to thank the whole H.E.S.S. and the GLAST-LAT collaborations for their support and helpful discussions on the topic, in particular Werner Hofmann, Felix Aharonian, Benoit Lott, and Seth Digel. DFT is supported by the Spanish MEC grant AYA 2006-00530, he acknowledges Juan Cortina and other members of the MAGIC collaboration for advice and encouragement. OR is supported by the National Aeronautics and Space Administration under contract NAS5-00147 with Stanford University. JAH is supported by an STFC Advanced Fellowship.

REFERENCES

- Abdo, A., et al., 2007, ApJ 664, 91
- Aharonian F.A., & Atayan, A.M. 1996, A&A 309, 91
- Aharonian, F. A., et al., 2001, A&A 370, 112
- Aharonian, F. A., et al. (*HEGRA Collaboration*), 2001, ApJ 614, 897
- Aharonian, F. A., et al. (*H.E.S.S. Collaboration*), 2005a, A&A 435, L17

- Aharonian, F. A., et al. (*H.E.S.S. Collaboration*), 2005b, *Science* 307, 1938
- Aharonian, F. A., et al. (*H.E.S.S. Collaboration*), 2005c, *A&A* 442, 1A
- Aharonian, F. A., et al. (*H.E.S.S. Collaboration*), 2006a, *A&A* 449, 223
- Aharonian, F. A., et al. (*H.E.S.S. Collaboration*), 2006b, *A&A* 460, 365
- Aharonian, F. A., et al. (*H.E.S.S. Collaboration*), 2006c, *A&A* 456, 245
- Aharonian, F. A., et al. (*H.E.S.S. Collaboration*), 2006d, *A&A* 460, 743
- Aharonian, F. A., et al. (*H.E.S.S. Collaboration*), 2006e, *Science* 312, 1771
- Aharonian, F. A., et al. (*H.E.S.S. Collaboration*), 2006f, *A&A* 457, 899
- Aharonian, F. A., et al. (*H.E.S.S. Collaboration*), 2006g, *ApJ* 636, 777
- Aharonian, F. A., et al. (*H.E.S.S. Collaboration*), 2007a, *A&A* 464, 235
- Aharonian, F. A., et al. (*H.E.S.S. Collaboration*), 2007b, *ApJ* 661, 236
- Aharonian, F. A., et al. (*H.E.S.S. Collaboration*), 2007c, *A&A* 467, 1075
- Aharonian, F. A., et al., (*H.E.S.S. Collaboration*), 2007d, *A&A* 466, 543
- Aharonian, F. A., et al., (*H.E.S.S. Collaboration*), 2007e, *A&A* 469, L1
- Albert, J., et al. (*MAGIC Collaboration*), 2006, *Science* 312, 1771
- Albert, J., et al. (*MAGIC Collaboration*), 2007a, submitted to *ApJ* (astro-ph/0705.3244)
- Albert, J., et al. (*MAGIC Collaboration*), 2007b, *ApJ* 664, 87
- Albert, J., et al. (*MAGIC Collaboration*), 2007c, *A&A* in press (astro-ph/0706.4065)
- Albert, J., et al. (*MAGIC Collaboration*), 2007d, *ApJ* 665, 51
- Atkins, R. et al., 2002, *NIM A* 449, 478
- Atkins, R., et al., 2003, *ApJ* 595, 803
- Atoyan A. M., Aharonian F. A., & Völk H. J. 1995, *Phys. Rev. D* 52, 3265
- Berge, D., Funk, S. & Hinton, J. A., 2007, *A&A* 466, 1219
- Bertsch, D. L. et al., Proc. 5th Compton Symposium, AIP Conf. Proc. 510, 2000, 504

- Blumenthal, G.R., & Gould, R.J., 1970, *RvMP.*, 42, Number 2, 237
- Braje, T. M. et al, 2000, *ApJ* 565, L91
- Carrigan, S., et al, 2007, *Proc. 30th International Cosmic Ray Conference*, Merida, Mexico, 2007
- D’Amico, N. et al., 2001, *ApJ*, 552, L45
- Dermer, C. D., & Böttcher, M. 2006, *ApJ* 644, 409
- Domingo-Santamaria E. & Torres D. F. 2006 *A&A* 448, 613
- Dubus G., 2006, *A&A* 451, 9
- Ellison, D. C., et al, 2007, *ApJ* 661, 879
- Esposito, J. A., Hunter, S. D., Kanbach, G., & Sreekumar, P., 1996, *ApJ* 461, 820
- Funk, S., 2005, PhD thesis, Ruprecht-Karls-Universität Heidelberg
(<http://www.ub.uni-heidelberg.de/archiv/5542>)
- Funk, S., 2006, *ApSS* 309, 11
- Funk, S., et al., 2007, *ApJ* 662, 517
- Funk, S., et al, 2007b, *Proc. 30th International Cosmic Ray Conference*, Merida, Mexico, 2007
- Gaensler, B. M., et al 2003, *ApJ*, 588, 441
- Ginzburg V.L., Syrovatskii S.I. 1964, “The Origin of Cosmic Rays”, Pergamon Press, London
- Hoppe, S., et al, 2007, *Proc. 30th International Cosmic Ray Conference*, Merida, Mexico, 2007
- Hartman, R. C., et al., 1999, *ApJS* 123, 79
- Kappes, A., et al, 2007, *ApJ* 656, 870
- Khangulyan, D., Aharonian, F., & Bosch-Ramon, V., submitted to *MNRAS* (astro-ph/0707.1689)
- Kniffen, D. A., et al., 1997, *ApJ* 486, 126

- Mattox, J. M., et al., 1996, ApJ 461, 396
- Moiseev, A., et al., 2007, APh 27, 339
- Nolan, P., et al., 1993, ApJ 409, 697
- Paredes, J. M., et al., Science 288, 2340
- Paredes, J. M., Bosch-Ramon, V., & Romero, G. E., 2006, A&A 451, 259
- Petry, D., 2001, ASSL 267, 299
- Protheroe, R. J., Mastichiadis, A., & Dermer, C. D., 1992, Aph 1, 113
- Reimer, O. & Bertsch, D.L., Proc. 27th ICRC, 2001, Vol.6, 2546
- Reimer, O., & Funk, S., 2007, Ap&SS 309, 203
- Romero, G. E., Benaglia, P., & Torres, D. F., 1999, A&A 348, 868
- Sierpowska-Bartosik A. & Torres D. F., 2007, submitted to ApJ (astro-ph/0708.0189)
- Smith, A., et al, 2007, Proc. 30th International Cosmic Ray Conference, Merida, Mexico, 2007
- Sturmer, S. J., & Dermer, C. D., 1995, A&A 293 (1), L17
- Tavani, M., et al., 1998, ApJ 497, L98
- Thompson, D .J. et al., 1994, Nature 359, 615
- Thompson, D. J., Bertsch, D. L., O’Neal, R. H., 2005, ApJs 157, 324
- Torres, D. F., Romero, G. E., Dame, T. M., Combi, J. A., & Butt, Y. M., 2003, PhR, 382, 303
- Torres D. F., Domingo-Santamaria E., & Romero G. E., 2004, ApJ 601, L75
- Wang, W., et al., 2005, MNRAS 360, 646
- T. C. Weekes et al., 1989, ApJ 342, 379
- Zdziarski, A. A., 1987, ApJ 335, 786